MOX-Report No. 25/2016

Hi-POD solution of parametrized fluid dynamics problems: preliminary results

Baroli, D.; Cova, C.M.; Perotto, S.; Sala, L.; Veneziani, A.

Hi-POD solution of parametrized fluid dynamics problems: preliminary results

Davide Baroli[♯,∗], Cristina Maria Cova[‡], Simona Perotto[♯],
Lorenzo Sala[‡], Alessandro Veneziani[♭]

July 11, 2016

[♯] MOX, Dipartimento di Matematica, Politecnico di Milano
Piazza Leonardo da Vinci 32, I-20133 Milano, Italy
davide.baroli@polimi.it, simona.perotto@polimi.it
[‡] Politecnico di Milano, Piazza Leonardo da Vinci 32, I-20133 Milano, Italy
cristina.cova@mail.polimi.it, lorenzo3.sala@mail.polimi.it
[♭] Department of Mathematics and Computer Science, Emory University
Atlanta, GA 30322, USA
ale@mathcs.emory.edu

Keywords: model reduction, POD, advection-diffusion-reaction problems, Navier-Stokes equations, modal expansion, finite elements.

Abstract

Numerical modeling of fluids in pipes or network of pipes (like in the circulatory system) has been recently faced with new methods that exploit the specific nature of the dynamics, so that a one dimensional axial mainstream is enriched by local secondary transverse components [4, 16, 18]. These methods - under the name of Hi-Mod approximation - construct a solution as a finite element axial discretization, completed by a spectral approximation of the transverse dynamics. It has been demonstrated that Hi-Mod reduction significantly accelerates the computations without compromising the accuracy. In view of variational data assimilation procedures (or, more in general, control problems), it is crucial to have efficient model reduction techniques to rapidly solve, for instance, a parametrized problem for several choices of the parameters of interest. In this work, we present some preliminary results merging Hi-Mod techniques with a classical Proper Orthogonal Decomposition (POD) strategy. We name this new approach as Hi-POD model reduction. We demonstrate the efficiency and the reliability of Hi-POD on multiparameter advection-diffusion-reaction problems as well as on the incompressible Navier-Stokes equations, both in a steady and in an unsteady setting.

[∗]Current affiliation : Faculté des Sciences, de la Technologie et de la Communication, Université du Luxembourg, 6, rue Richard Coudenhove-Kalergi, L-1359 Luxembourg

1 Introduction

The growing request of efficient and reliable numerical simulations for modeling, designing and optimizing engineering systems in a broad sense, challenges traditional methods for solving partial differential equations (PDEs). While general purpose methods like finite elements are suitable for high fidelity solutions of direct problems, practical applications often require to deal with multi-query settings, where the right balance between accuracy and efficiency becomes critical. Customization of methods to exploit all the possible features of the problem at hand may yield significant improvements in terms of efficiency, possibly with no meaningful loss in the accuracy required by engineering problems.

In this paper we focus on parametrized PDEs to model incompressible fluid dynamic problems in pipes or elongated domains. In particular, we propose to combine the Hi-Mod reduction technique, which is customized on problems featuring a leading dynamics triggered by the geometry, with a standard POD approach for a rapid solution of parametrized settings.

A Hi-Mod approximation represents a fluid in a pipe as a one-dimensional mainstream, locally enriched via transverse components. This separate description of dynamics leads to construct psychological 1D models, yet able of switching to a locally higher fidelity [4, 15, 16, 18, 19]. The rationale behind a Hi-Mod approach is that a 1D classical model can be effectively improved by a spectral approximation of transverse components. In fact, the high accuracy of spectral methods guarantees, in general, that a low number of modes suffices to obtain a reliable approximation, yet with contained computational costs.

POD is a popular strategy in design, assimilation and optimization contexts, and relies on the so-called offline-online paradigm [7, 8, 10, 23, 26]. The offline stage computes the (high fidelity) solution to the problem at hand for a set of samples of the selected parameters. Then, an educated basis (called POD basis) is built by optimally extracting the most important components of the offline solutions (called snapshots), collected in the so-called response matrix, via a singular value decomposition. Finally, in the online phase, the POD basis is used to efficiently represent the solution associated with new values of the parameters of interest, *a priori* unknown.

In the Hi-POD procedure, the Hi-Mod reduction is used to build the response matrix during the offline stage. Then, we perform the online computation by assembling the Hi-Mod matrix associated with the new parameter and, successively, by projecting such a matrix onto the POD basis. As we show in this work, Hi-POD demonstrates to be quite competitive on a set of multiparameter problems, including linear scalar advection-diffusion-reaction problems and the incompressible Navier-Stokes equations.

The paper is organized as follows. In Section 2, we detail the Hi-POD technique and we apply it to an advection-diffusion-reaction problem featuring six parameters, pinpointing the efficiency of the procedure. Section 3 generalizes Hi-POD to a vector problem, by focusing on the steady incompressible Navier-

Stokes equations, while the unsteady case is covered in Section 4. Some conclusions are drawn in Section 5, where some hints for a possible future investigation are also provided.

2   Hi-POD reduction of parametrized PDEs: basics

Merging of Hi-Mod and POD procedures for parametrized PDEs has been proposed in [12, 13], in what we called *Hi-POD method*. We briefly recall the two ingredients, separately. Then, we illustrate a basic example of Hi-POD technique.

2.1   The Hi-Mod setting

Let $\Omega \subset \mathbb{R}^d$ be a d-dimensional domain, with $d = 2, 3$, that makes sense to represent as $\Omega \equiv \bigcup_{x \in \Omega_{1D}} \{x\} \times \Sigma_x$, where Ω_{1D} is the $1D$ horizontal supporting fiber, while $\Sigma_x \subset \mathbb{R}^{d-1}$ represents the transverse section at $x \in \Omega_{1D}$. The reference morphology is a pipe, where the dominant dynamics occurs along Ω_{1D}. We generically consider an elliptic problem in the form

$$\text{find } u \in V : a(u, v) = F(v) \quad \forall v \in V, \tag{1}$$

where $V \subseteq H^1(\Omega)$ is a Hilbert space, $a(\cdot, \cdot) : V \times V \to \mathbb{R}$ is a coercive, continuous bilinear form and $F(\cdot) : V \to \mathbb{R}$ is a linear and continuous form. Standard notation for the function spaces is adopted [11]. We refer to u in (1) as to the *full solution*. The solution to this problem is supposed to depend on some parameters that we will highlight in our notation later on.

In the Hi-Mod reduction procedure, we introduce the space

$$V_m^h = \left\{ v_m^h(x, \mathbf{y}) = \sum_{k=1}^m \tilde{v}_k^h(x) \varphi_k(\mathbf{y}), \text{ with } \tilde{v}_k^h \in V_{1D}^h, \ x \in \Omega_{1D}, \ \mathbf{y} \in \Sigma_x \right\},$$

where $V_{1D}^h \subset H^1(\Omega_{1D})$ is a discrete space of size N_h, $\{\varphi_k\}_{k \in \mathbb{N}^+}$ is a basis of L^2-orthonormal modal functions to describe the dynamics in Σ_x, for x varying along Ω_{1D}. For more details about the choice of the modal basis, we refer to [1, 3, 16], while V_{1D}^h may be a classical finite element space [4, 16, 18, 19] or an isogeometric function space [17].

The modal index $m \in \mathbb{N}^+$ determines the level of detail of the Hi-Mod reduced model. It may be fixed *a priori*, driven by some preliminary knowledge of the phenomenon at hand as in [4, 16], or automatically chosen via an *a posteriori* modeling error analysis as in [18, 20]. Index m can be varied along the domain to better capture local dynamics [19, 20]. For simplicity, here we consider m to be given and constant along the whole domain (*uniform* Hi-Mod reduction).

For a given modal index $m \in \mathbb{N}^+$, the Hi-Mod formulation reads as

$$\text{find } u_m^h \in V_m^h : a(u_m^h, v_m^h) = F(v_m^h) \quad \forall v_m^h \in V_m^h. \tag{2}$$

The well-posedness of formulation (2) as well as the convergence of u_m^h to u can be proved under suitable assumptions on space V_m^h [16].

In particular, after denoting by $\{\vartheta_j\}_{j=1}^{N_h}$ a basis of the space V_{1D}^h, for each element $v_m^h \in V_m^h$, the Hi-Mod expansion reads

$$v_m^h(x, \mathbf{y}) = \sum_{k=1}^{m} \Big[\sum_{j=1}^{N_h} \tilde{v}_{k,j} \vartheta_j(x) \Big] \varphi_k(\mathbf{y}).$$

The unknowns of (2) are the mN_h coefficients $\big\{ \tilde{u}_{k,j} \big\}_{j=1,k=1}^{N_h, m}$ identifying the Hi-Mod solution u_m^h. The Hi-Mod reduction obtains a system of m coupled "psychologically" 1D problems. For m small (i.e., when the mainstream dominates the dynamics), the solution process competes with purely 1D numerical models. Accuracy of the model can be improved locally by properly setting m. From an algebraic point of view, we solve the linear system $A_m^h \mathbf{u}_m^h = \mathbf{f}_m^h$, where $A_m^h \in \mathbb{R}^{mN_h \times mN_h}$ is the Hi-Mod stiffness matrix, $\mathbf{u}_m^h \in \mathbb{R}^{mN_h}$ is the vector of the Hi-Mod coefficients and $\mathbf{f}_m^h \in \mathbb{R}^{mN_h}$ is the Hi-Mod right-hand side.

2.2 POD solution of parametrized Hi-Mod problems

Let us denote by $\boldsymbol{\alpha}$ a vector of parameters the solution of problem (1) depends on. We reflect this dependence in our notation by writing the Hi-Mod solution as

$$u_m^h(\boldsymbol{\alpha}) = u_m^h(x, \mathbf{y}, \boldsymbol{\alpha}) = \sum_{k=1}^{m} \Big[\sum_{j=1}^{N_h} \tilde{u}_{k,j}^{\boldsymbol{\alpha}} \vartheta_j(x) \Big] \varphi_k(\mathbf{y}), \tag{3}$$

corresponding to the algebraic Hi-Mod system

$$A_m^h(\boldsymbol{\alpha}) \mathbf{u}_m^h(\boldsymbol{\alpha}) = \mathbf{f}_m^h(\boldsymbol{\alpha}). \tag{4}$$

The Hi-Mod approximation to problem (1) will be indifferently denoted via (3) or by the vector $\mathbf{u}_m^h(\boldsymbol{\alpha})$.

The goal of the Hi-POD procedure that we describe hereafter is to rapidly estimate the solution to (1) for a specific set $\boldsymbol{\alpha}^*$ of data, by exploiting Hi-Mod solutions previously computed for different choices of the parameter vector. The rationale is to reduce the computational cost of the solution to (4), yet preserving reliability.

According to the POD approach, we exploit an offline/online paradigm, i.e.,

- we compute the Hi-Mod approximation associated with different samples of the parameter $\boldsymbol{\alpha}$ to build the POD reduced basis (*offline phase*);

- we compute the solution for $\boldsymbol{\alpha}^*$ by projecting system (4) onto the space spanned by the POD basis (*online phase*).

2.2.1 The offline phase

We generate the reduced POD basis relying on a set of available samples of the solution computed with the Hi-Mod reduction. Even though off-line costs are not usually considered in evaluating the advantage of a POD procedure, also this stage may introduce a computational burden when many samples are needed, like in multiparametric problems. The generation of snapshots with the Hi-Mod approach, already demonstrated to be significantly faster [3], mitigates the costs of this phase. The pay-off of the procedure is based on the expectation that the POD basis is considerably lower-size than the order mN_h of the Hi-Mod system. We will discuss this aspect in the numerical assessment.

Let S be the so-called *response matrix*, collecting p Hi-Mod solutions to (1), for p different values $\boldsymbol{\alpha}_i$ of the parameter, with $i = 1, \ldots, p$. Precisely, we identify each Hi-Mod solution with the corresponding vector in (4),

$$\mathbf{u}_m^h(\boldsymbol{\alpha}_i) = \left[\tilde{u}_{1,1}^{\boldsymbol{\alpha}_i}, \ldots, \tilde{u}_{1,N_h}^{\boldsymbol{\alpha}_i}, \tilde{u}_{2,1}^{\boldsymbol{\alpha}_i}, \ldots, \tilde{u}_{2,N_h}^{\boldsymbol{\alpha}_i}, \ldots, \tilde{u}_{m,N_h}^{\boldsymbol{\alpha}_i}\right]^T \in \mathbb{R}^{mN_h}, \qquad (5)$$

the unknown coefficients being ordered mode-wise. Thus, the response (or snapshot) matrix $S \in \mathbb{R}^{(mN_h) \times p}$ reads

$$S = \left[\mathbf{u}_m^h(\boldsymbol{\alpha}_1), \mathbf{u}_m^h(\boldsymbol{\alpha}_2), \ldots, \mathbf{u}_m^h(\boldsymbol{\alpha}_p)\right] = \begin{bmatrix} \tilde{u}_{1,1}^{\boldsymbol{\alpha}_1} & \tilde{u}_{1,1}^{\boldsymbol{\alpha}_2} & \ldots & \tilde{u}_{1,1}^{\boldsymbol{\alpha}_p} \\ \vdots & \vdots & \vdots & \vdots \\ \tilde{u}_{1,N_h}^{\boldsymbol{\alpha}_1} & \tilde{u}_{1,N_h}^{\boldsymbol{\alpha}_2} & \ldots & \tilde{u}_{1,N_h}^{\boldsymbol{\alpha}_p} \\ \tilde{u}_{2,1}^{\boldsymbol{\alpha}_1} & \tilde{u}_{2,1}^{\boldsymbol{\alpha}_2} & \ldots & \tilde{u}_{2,1}^{\boldsymbol{\alpha}_p} \\ \vdots & \vdots & \vdots & \vdots \\ \tilde{u}_{2,N_h}^{\boldsymbol{\alpha}_1} & \tilde{u}_{2,N_h}^{\boldsymbol{\alpha}_2} & \ldots & \tilde{u}_{2,N_h}^{\boldsymbol{\alpha}_p} \\ \vdots & \vdots & \vdots & \vdots \\ \tilde{u}_{m,N_h}^{\boldsymbol{\alpha}_1} & \tilde{u}_{m,N_h}^{\boldsymbol{\alpha}_2} & \ldots & \tilde{u}_{m,N_h}^{\boldsymbol{\alpha}_p} \end{bmatrix}. \qquad (6)$$

The selection of representative values of the parameter is clearly critical in the effectiveness of the POD procedure. More the snapshots cover the entire parameter space and more evident the model reduction will be. This is a non-trivial issue, generally problem dependent. For instance, in [9] the concept of *domain of effectiveness* is introduced to formalize the region of the parameter space accurately covered by a snapshot in a problem of cardiac conductivity. In this preliminary work, we do not dwell with this aspect since we work on more general problems. A significant number of snapshots is anyhow needed to construct an efficient POD basis, the Hi-Mod procedure providing an effective tool for this purpose (with respect to a full finite element generation of the snapshots).

To establish a correlation between the POD procedure and statistical mo-

ments, we enforce the snapshot matrix to have null average by setting

$$R = S - \frac{1}{p}\sum_{i=1}^{p} \begin{bmatrix} \tilde{u}_{1,1}^{\boldsymbol{\alpha}_i} & \tilde{u}_{1,1}^{\boldsymbol{\alpha}_i} & \cdots & \tilde{u}_{1,1}^{\boldsymbol{\alpha}_i} \\ \vdots & \vdots & \vdots & \vdots \\ \tilde{u}_{1,N_h}^{\boldsymbol{\alpha}_i} & \tilde{u}_{1,N_h}^{\boldsymbol{\alpha}_i} & \cdots & \tilde{u}_{1,N_h}^{\boldsymbol{\alpha}_i} \\ \tilde{u}_{2,1}^{\boldsymbol{\alpha}_i} & \tilde{u}_{2,1}^{\boldsymbol{\alpha}_i} & \cdots & \tilde{u}_{2,1}^{\boldsymbol{\alpha}_i} \\ \vdots & \vdots & \vdots & \vdots \\ \tilde{u}_{2,N_h}^{\boldsymbol{\alpha}_i} & \tilde{u}_{2,N_h}^{\boldsymbol{\alpha}_i} & \cdots & \tilde{u}_{2,N_h}^{\boldsymbol{\alpha}_i} \\ \vdots & \vdots & \vdots & \vdots \\ \tilde{u}_{m,N_h}^{\boldsymbol{\alpha}_i} & \tilde{u}_{m,N_h}^{\boldsymbol{\alpha}_i} & \cdots & \tilde{u}_{m,N_h}^{\boldsymbol{\alpha}_i} \end{bmatrix} \in \mathbb{R}^{(mN_h)\times p}. \tag{7}$$

By Singular Value Decomposition (SVD), we write

$$R = \Psi \Sigma \Phi^T,$$

with $\Psi \in \mathbb{R}^{(mN_h)\times(mN_h)}$, $\Sigma \in \mathbb{R}^{(mN_h)\times p}$, $\Phi \in \mathbb{R}^{p\times p}$. Matrices Ψ and Φ are unitary and collect the left and the right singular vectors of R, respectively. Matrix $\Sigma = \text{diag}\,(\sigma_1,\dots,\sigma_q)$ is pseudo-diagonal, $\sigma_1,\sigma_2,\dots,\sigma_q$ being the singular values of R, with $\sigma_1 \geq \sigma_2 \geq \cdots \geq \sigma_q$ and $q = \min\{mN_h,p\}$ [6]. In the numerical assessment below, we take $q = p$.

The POD (orthogonal) basis is given by the l left singular vectors $\{\boldsymbol{\psi}_i\}$ associated with the most significant l singular values, with $l \ll mN_h$. Different criteria can be pursued to select those singular values. A possible approach is to select the first l ordered singular values, such that $\sum_{i=1}^{l}\sigma_i^2/\sum_{i=1}^{q}\sigma_i^2 \geq \varepsilon$ for a positive user-defined tolerance ε [26]. The reduced POD space then reads $V_{\text{POD}}^l = \text{span}\{\boldsymbol{\psi}_1,\dots,\boldsymbol{\psi}_l\}$, with $\dim(V_{\text{POD}}^l) = l$.

Equivalently, we can identify the POD basis by applying the spectral decomposition to the covariance matrix $C \equiv R^T R$ (being $mN_h \geq p$). As well known, the right singular vectors of R coincide with the eigenvectors $\mathbf{c}_i$ of C, with eigenvalues $\lambda_i = \sigma_i^2$, for $i = 1,\dots,p$. Thus, the POD basis functions reads $\boldsymbol{\psi}_i = \lambda_i^{-1} S\mathbf{c}_i$ [26].

2.2.2 The online phase

We aim at rapidly computing the Hi-Mod approximation to problem (1) for the parameter value $\boldsymbol{\alpha}^*$ not included in the sampling set $\{\boldsymbol{\alpha}_i\}_{i=1}^p$. For this purpose, we project the Hi-Mod system (4), with $\boldsymbol{\alpha} = \boldsymbol{\alpha}^*$, onto the POD space V_{POD}^l, by solving the linear system

$$A_{\text{POD}}^{\boldsymbol{\alpha}^*}\mathbf{u}_{\text{POD}}^{\boldsymbol{\alpha}^*} = \mathbf{f}_{\text{POD}}^{\boldsymbol{\alpha}^*},$$

with $A_{\text{POD}}^{\boldsymbol{\alpha}^*} = (\Psi_{\text{POD}}^l)^T A_m^h(\boldsymbol{\alpha}^*)\,\Psi_{\text{POD}}^l \in \mathbb{R}^{l\times l}$, $\mathbf{f}_{\text{POD}}^{\boldsymbol{\alpha}^*} = (\Psi_{\text{POD}}^l)^T \mathbf{f}_m^h(\boldsymbol{\alpha}^*) \in \mathbb{R}^l$ and $\mathbf{u}_{\text{POD}}^{\boldsymbol{\alpha}^*} = [u_{\text{POD},1}^{\boldsymbol{\alpha}^*},\dots,u_{\text{POD},l}^{\boldsymbol{\alpha}^*}]^T \in \mathbb{R}^l$, where $A_m^h(\boldsymbol{\alpha}^*)$ and $\mathbf{f}_m^h(\boldsymbol{\alpha}^*)$ are defined as in (4), and $\Psi_{\text{POD}}^l = [\boldsymbol{\psi}_1,\dots,\boldsymbol{\psi}_l] \in \mathbb{R}^{(mN_h)\times l}$ is the matrix collecting, by column, the POD basis functions.

By exploiting the POD basis, we write

$$\mathbf{u}_m^h(\boldsymbol{\alpha}^*) \approx \sum_{s=1}^{l} u_{\text{POD},s}^{\boldsymbol{\alpha}^*} \boldsymbol{\psi}_s.$$

The construction of $A_{\text{POD}}^{\boldsymbol{\alpha}^*}$ and $\mathbf{f}_{\text{POD}}^{\boldsymbol{\alpha}^*}$ requires the assembly of the Hi-Mod matrix/right-hand side for the value $\boldsymbol{\alpha}^*$, successively projected onto the POD space. Also in the basic POD online phase, we need to assembly, in general, the full problem, and the Hi-Mod model, featuring lower size than a full finite element problem, gives a computational advantage. In addition, the final solution is computed by solving an $l \times l$ system as opposed to the $mN_h \times mN_h$ Hi-Mod system, with a clear overall computational advantage, as we verify hereafter.

2.3   Numerical assessment

In this preliminary paper, we consider only 2D problems, the 3D case being a development of the present work. We consider the linear advection-diffusion-reaction (ADR) problem

$$\begin{cases} -\nabla \cdot \big(\mu(\mathbf{x})\nabla u(\mathbf{x})\big) + \mathbf{b}(\mathbf{x}) \cdot \nabla u(\mathbf{x}) + \sigma(\mathbf{x})u(\mathbf{x}) = f(\mathbf{x}) & \text{in } \Omega \\ u(\mathbf{x}) = 0 & \text{on } \Gamma_D \\ \mu(\mathbf{x})\dfrac{\partial u}{\partial n}(\mathbf{x}) = 0 & \text{on } \Gamma_N, \end{cases} \tag{8}$$

with $\Gamma_D, \Gamma_N \subset \partial\Omega$, such that $\Gamma_D \cup \Gamma_N = \partial\Omega$ and $\overset{\circ}{\Gamma}_D \cap \overset{\circ}{\Gamma}_N = \emptyset$, where μ, $\mathbf{b}$, σ and f denote the viscosity, the advective field, the reactive coefficient and the source term, respectively. In particular, we set $\Omega = (0,6) \times (0,1)$, with $\Gamma_N = \{(x,y) : x = 6, 0 \le y \le 1,\}$ and $\Gamma_D = \partial\Omega \setminus \Gamma_N$. We also assume constant viscosity and reaction, i.e., we pick $\mu = 0.1\mu_0$ for $\mu_0 \in [1,10]$ and $\sigma \in [0,3]$; then, we assign a sinusoidal advective field, $\mathbf{b}(\mathbf{x}) = [b_1, b_2 \sin(6x)]^T$ with $b_1 \in [2,20]$ and $b_2 \in [1,3]$, and the source term $f(\mathbf{x}) = f_1\chi_{C_1}(\mathbf{x}) + f_2\chi_{C_2}(\mathbf{x})$ for f_1, $f_2 \in [5,25]$ and where function χ_ω denotes the characteristic function associated with the generic domain ω, $C_1 = \{(x,y) : (x-1.5)^2 + 0.4\,(y-0.25)^2 < 0.01\}$ and $C_2 = \{(x,y) : (x-0.75)^2 + 0.4\,(y-0.75)^2 < 0.01\}$ identifying two ellipsoidal areas in Ω. According to the notation in (1), we set therefore $V \equiv H^1_{\Gamma_D}(\Omega)$, $a(u,v) \equiv \big(\mu\nabla u, \nabla v\big) + \big(\mathbf{b} \cdot \nabla u + \sigma u, v\big)$, for any $u, v \in V$, and $F(v) = \big(f, v\big)$, for any $v \in V$, $(\cdot, \cdot)$ denoting the $L^2(\Omega)$-scalar product.

In the offline phase, we select $p = 30$ problems, by *randomly* varying coefficients μ_0, σ, b_1, b_2, f_1 and f_2 in the corresponding ranges, so that $\boldsymbol{\alpha} \equiv [\mu_0, \sigma, b_1, b_2, f_1, f_2]^T$. We introduce a uniform partition of Ω_{1D} into 121 subintervals, and we Hi-Mod approximate the selected p problems, combining piecewise linear finite elements along the 1D fiber with a modal expansion based on 20 sinusoidal functions along the transverse direction.

In the online phase, we aim at computing the Hi-Mod approximation to problem (8) for $\boldsymbol{\alpha} = \boldsymbol{\alpha}^* = [\mu_0^*, \sigma^*, b_1^*, b_2^*, f_1^*, f_2^*]^T$, with

$$\mu_0^* = 2.4, \quad \sigma^* = 0, \quad b_1^* = 5, \quad b_2^* = 1, \quad f_1^* = f_2^* = 10.$$

Figure 1 shows a Hi-Mod reference solution, $u_m^{R,h}$, computed by directly applying Hi-Mod reduction to (8) for $\boldsymbol{\alpha} = \boldsymbol{\alpha}^*$, with the same Hi-Mod discretization setting used for the offline phase.

This test is intended to demonstrate the reliability of Hi-POD to construct an approximation of the Hi-Mod solution (that, in turn, approximates the full solution u), with a contained computational cost.

Figure 2 shows the spectrum of the response matrix R in (7). As highlighted by the vertical lines, we select four different values for the number l of POD modes, i.e., $l = 2, 6, 19, 29$. For these choices, the ratio $\sum_{i=1}^{l} \sigma_i^2 / \sum_{i=1}^{q} \sigma_i^2$ assumes the value 0.780 for $l = 2$, 0.971 for $l = 6$, 0.999 for $l = 19$ (and, clearly, 1 for $l = 29$). The singular values for the specific problem decay quite slowly. This is due to the presence of many (six) parameters, so that the redundancy of the snapshots (that triggers the decay) is quite limited.

Nevertheless, we observe that the Hi-POD solution still furnishes a reliable and rapid approximation of the solution in correspondence of the value $\boldsymbol{\alpha}^*$. Precisely, Figure 3 shows the Hi-Mod approximation provided by Hi-POD, for $l = 2, 6, 19$ (top-bottom). We stress that six POD modes are enough to obtain a Hi-Mod reduced solution which, qualitatively, exhibits the same features as $u_m^{R,h}$. Moreover, the contribution of singular vectors for $l > 19$ is of no improvement. We also notice that the results for $l = 6$ are excellent, since six scalar parameters influence the solution.
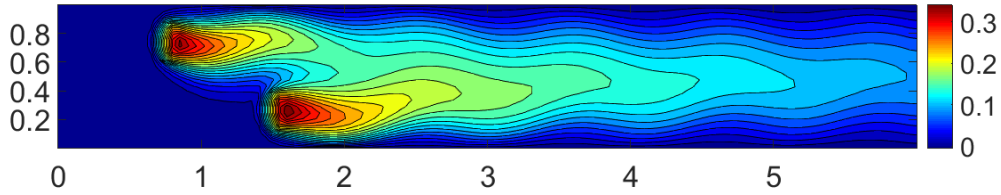

Figure 1: ADR problem. Hi-Mod reference solution.

Table 1 provides more quantitative information. We collect the $L^2(\Omega)$- and the $H^1(\Omega)$-norm of the relative error obtained by replacing the Hi-Mod reference solution with the one provided by the Hi-POD approach. As expected, the error diminishes proportionally to the number of POD modes.
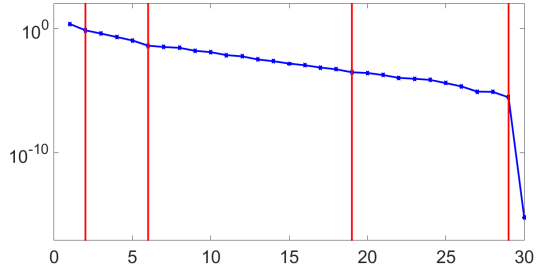
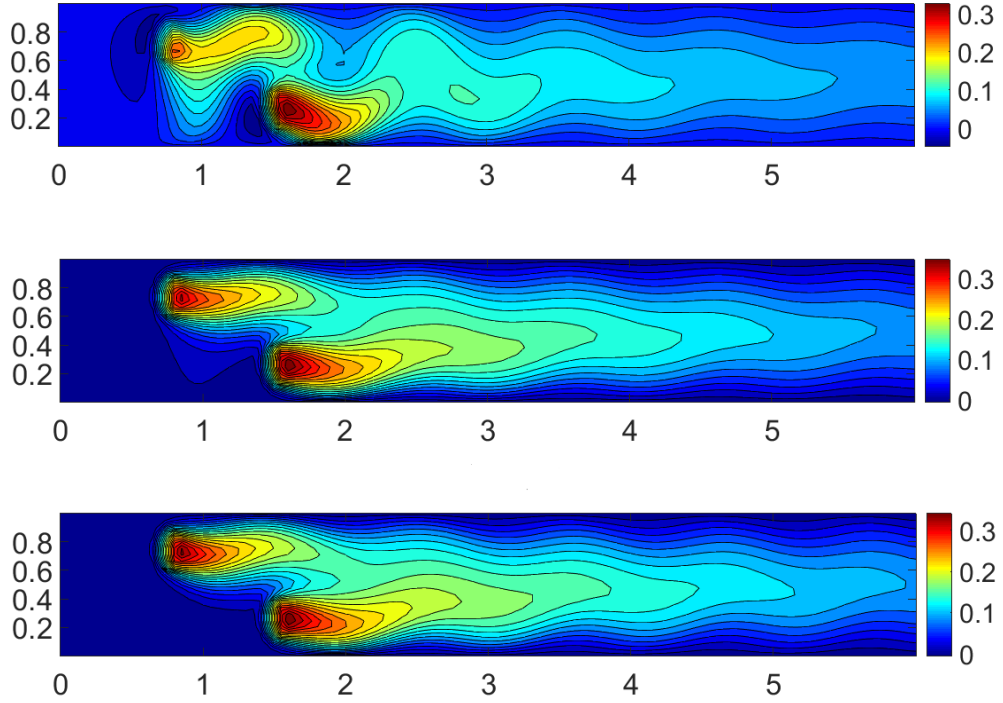Figure 2: ADR problem. Singular values of the response matrix R.

Figure 3: ADR problem. Hi-Mod approximation provided by the Hi-POD approach for $l = 2$ (top), $l = 6$ (center), $l = 19$ (bottom).

3 Hi-POD reduction of the Navier-Stokes equations

We generalize the Hi-POD procedure in Section 2.2 to the incompressible Navier-Stokes equations [25]. We first consider the stationary problem

$$
\begin{cases}
-\nabla \cdot (2\nu \, \mathbb{D}(\mathbf{u}))\,(\mathbf{x}) + (\mathbf{u} \cdot \nabla)\,\mathbf{u}(\mathbf{x}) + \nabla p(\mathbf{x}) = \mathbf{f}(\mathbf{x}) & \text{in } \Omega \\
\nabla \cdot \mathbf{u}(\mathbf{x}) = 0 & \text{in } \Omega \\
\mathbf{u}(\mathbf{x}) = \mathbf{0} & \text{on } \Gamma_D \\
(\mathbb{D}(\mathbf{u}) - p\mathbb{I})\,(\mathbf{x})\,\mathbf{n} = g\mathbf{n} & \text{on } \Gamma_N,
\end{cases}
\tag{9}
$$

9

	$l = 2$	$l = 6$	$l = 19$	$l = 29$
$\dfrac{\|u_m^{R,h} - u_m^h(\boldsymbol{\alpha}^*)\|_{L^2(\Omega)}}{\|u_m^{R,h}\|_{L^2(\Omega)}}$	3.52e-01	3.44e-02	9.71e-04	4.38e-04
$\dfrac{\|u_m^{R,h} - u_m^h(\boldsymbol{\alpha}^*)\|_{H^1(\Omega)}}{\|u_m^{R,h}\|_{H^1(\Omega)}}$	4.54e-01	6.88e-02	2.21e-03	8.24e-04

Table 1: ADR problem. Relative errors for different Hi-POD reconstructions of the Hi-Mod solution.

with $\mathbf{u} = [u_1, u_2]^T$ and p the velocity and the pressure of the flow, respectively $\nu > 0$ the kinematic viscosity, $\mathbb{D}(\mathbf{u}) = \frac{1}{2}\left(\nabla\mathbf{u} + (\nabla\mathbf{u})^T\right)$ the strain rate, $\mathbf{f}$ the force per unit mass, $\mathbf{n}$ the unit outward normal vector to the domain boundary $\partial\Omega$, $\mathbb{I}$ the identity tensor, g a sufficiently regular function, and where Γ_D and Γ_N are defined as in (8). We apply a standard Picard linearization of the nonlinear term

$$
\begin{cases}
-\nabla \cdot \left(2\nu\,\mathbb{D}(\mathbf{u}^{k+1})\right) + \left(\mathbf{u}^k \cdot \nabla\right)\mathbf{u}^{k+1} + \nabla p^{k+1} = \mathbf{f} & \text{in } \Omega \\
\nabla \cdot (\mathbf{u}^{k+1}) = 0 & \text{in } \Omega \\
\mathbf{u}^{k+1} = \mathbf{0} & \text{on } \Gamma_D \\
\left(\mathbb{D}(\mathbf{u}^{k+1}) - p^{k+1}\mathbb{I}\right)\mathbf{n} = g\mathbf{n} & \text{on } \Gamma_N,
\end{cases}
$$

where $\{\mathbf{u}^j, p^j\}$ denotes the unknown pair at the iteration j. Stopping criterion of the Picard iteration is designed on the increment between two consecutive iterations.

Problem (9) is approximated via a standard Hi-Mod technique, for both the velocity and the pressure, where a modal basis constituted by orthogonal Legendre polynomials, adjusted to include the boundary conditions, is used. Finite elements are used along the centerline. The finite dimension Hi-Mod spaces for velocity and pressure obtained by the combination of different discretization methods need to be inf-sup compatible. Unfortunately, no proof of compatibility is currently available, even though some empirical strategies based on the Bathe-Chapelle test are available [3, 5]. In particular, here we take piecewise quadratic velocity/linear pressure along the mainstream and the numbers $m_p, m_{\mathbf{u}}$ of pressure and velocity modes is set such that $m_{\mathbf{u}} = m_p + 2$. Numerical evidence suggests this to be an inf-sup compatible choice [2, 5]. Finally, the same number of modes is used for the two velocity components, for the sake of simplicity.

We denote by $V_{1D}^{h,u} \subset H^1(\Omega_{1D})$ and by $V_{1D}^{h,p} \subset L^2(\Omega_{1D})$ the finite element space adopted to discretize u_1, u_2 and p, respectively along Ω_{1D}, with $\dim(V_{1D}^{h,u}) = N_{h,u}$ and $\dim(V_{1D}^{h,p}) = N_{h,p}$. Thus, the total number of degrees of freedom involved by a Hi-Mod approximation of $\mathbf{u}$ and p is $N_{\mathbf{u}} = 2m_{\mathbf{u}}N_{h,u}$ and $N_p = m_p N_{h,p}$, respectively.

From an algebraic viewpoint, at each Picard iteration, we solve the linear system (we omit index k for easiness of notation)

$$
S_{\{m_{\mathbf{u}}, m_p\}}^h\, \mathbf{z}_{m_{\mathbf{u}}, m_p}^h = \mathbf{F}_{\{m_{\mathbf{u}}, m_p\}}^h, \tag{10}
$$

where

$$S_{\{m_\mathbf{u}, m_p\}}^h = \begin{bmatrix} C_{\{m_\mathbf{u}, m_\mathbf{u}\}}^h & [B_{\{m_\mathbf{u}, m_p\}}^h]^T \\ B_{\{m_\mathbf{u}, m_p\}}^h & 0 \end{bmatrix} \in \mathbb{R}^{(N_\mathbf{u} + N_p) \times (N_\mathbf{u} + N_p)},$$

with $C_{\{m_\mathbf{u}, m_\mathbf{u}\}}^h \in \mathbb{R}^{N_\mathbf{u} \times N_\mathbf{u}}$, $B_{\{m_\mathbf{u}, m_p\}}^h \in \mathbb{R}^{N_p \times N_\mathbf{u}}$ the Hi-Mod momentum and divergence matrix, respectively, $\mathbf{z}_{m_\mathbf{u}, m_p}^h = [\mathbf{u}_{m_\mathbf{u}}^h, p_{m_p}^h]^T \in \mathbb{R}^{N_\mathbf{u} + N_p}$ the vector of the Hi-Mod solutions, and where $\mathbf{F}_{\{m_\mathbf{u}, m_p\}}^h = [\mathbf{f}_{m_\mathbf{u}}^h, \mathbf{0}]^T \in \mathbb{R}^{N_\mathbf{u} + N_p}$, with $\mathbf{f}_{m_\mathbf{u}}^h$ the Hi-Mod right-hand side of the momentum equation.

When coming to the Hi-POD procedure for problem (9), we follow a segregated procedure, where a basis function set is constructed for the velocity and another one for the pressure. The effectiveness of this reduced basis in representing the solution for a different value of the parameter is higher with respect to a monolithic approach, where a unique POD basis is built. We will support this statement with numerical evidence. Still referring to (6)-(7), we build two separate response matrices, $R_\mathbf{u} \in \mathbb{R}^{N_\mathbf{u} \times p}$ and $R_p \in \mathbb{R}^{N_p \times p}$, which gather, by column, the Hi-Mod approximation for the velocity, $\mathbf{u}_{m_\mathbf{u}}^h(\boldsymbol{\alpha}) \in \mathbb{R}^{N_\mathbf{u}}$, and for the pressure, $p_{m_p}^h(\boldsymbol{\alpha}) \in \mathbb{R}^{N_p}$, solutions to the Navier-Stokes problem (9) for p different choices $\boldsymbol{\alpha}_i$, with $i = 1, \ldots, p$, of the parameter that, in this case, is $\boldsymbol{\alpha} = [\nu, \mathbf{f}, g]^T$. A standard block-Gaussian procedure resorting to the pressure Schur-complement is used to compute velocity and pressure, separately [24].

Following a segregated SVD analysis of the two unknowns, after identifying the two indices l_u and l_p, separately, we construct a unique reduced POD space V_{POD}^l, with $l = \max(l_u, l_p)$, by collecting the first l singular vectors of $R_\mathbf{u}$ and of R_p. More precisely, for a new value $\boldsymbol{\alpha}^*$ of the parameters, with $\boldsymbol{\alpha}^* \neq \boldsymbol{\alpha}_i$ for $i = 1, \ldots, p$, at each Picard iteration, we project the linearized Navier-Stokes problem onto the space V_{POD}^l.

Another possible approach is to keep the computation of the velocity and pressure separate on the two basis function sets with size l_u and l_p, by resorting to an approximation of the pressure Schur complement, followed by the computation of the velocity, similar to what is done in algebraic splittings [22, 24, 27, 28]. More in general, the treatment of the nonlinear term in the Navier-Stokes problem can follow approximation strategies with a specific basis function set and *empirical interpolation strategies* [23]. At this preliminary stage, we do not follow this approach and we just assess the performances of the basic procedure. However, this topic will be considered in the follow-up of the present work in view of real applications.

It is also worth noting that no inf-sup compatibility is guaranteed for the POD basis functions. Numerical evidence suggests that we do have inf-sup compatible basis functions, however a theoretical analysis is still missing.

3.1 A benchmark test case

We solve problem (9) on the rectangular domain $\Omega = (0, 8) \times (-2, 2)$, where $\Gamma_D = \{(x, y) : 0 \leq x \leq 8, y = \pm 2\}$ and $\Gamma_N = \partial \Omega \setminus \Gamma_D$.

Moreover, we assume the analytical representation

$$\mathbf{f} = \begin{bmatrix} f_{0,x} + f_{xx}\, x + f_{xy}\, y \\ f_{0,y} + f_{yx}\, x + f_{yy}\, y \end{bmatrix} \tag{11}$$

for the forcing term $\mathbf{f}$ involved in the parameter $\boldsymbol{\alpha}$.

In the offline stage, we Hi-Mod approximate $p = 30$ problems, by varying the coefficients f_{st}, for $s = 0, x, y$ and $t = x, y$, in (11), the kinematic viscosity ν and the boundary value g in (9). In particular, we randomly sample the coefficients f_{st} on the interval $[0, 100]$, whereas we adopt a uniform sampling for ν on $[30, 70]$ and for g on $[1, 80]$.

Concerning the adopted Hi-Mod discretization, we partition the fiber Ω_{1D} into 80 uniform sub-intervals to employ quadratic and linear finite elements for the velocity and the pressure, respectively. Five Legendre polynomials are used to describe the transverse trend of $\mathbf{u}$, while three modal functions are adopted for p.

In the online phase, we compute the Hi-POD approximation to problem (9) with parameters $\boldsymbol{\alpha}^* = [\mathbf{f}^*, \nu^*, g^*]^T$, with $\mathbf{f}^* = [82.6, 12.1]^T$, $\nu^* = 51.4$ and $g^* = 24.2$, $f_{xx} = f_{yy} = f_{xy} = f_{yx} = 0$. Figure 4 (left) shows the contour plots of the two components of the velocity and of the pressure for the reference Hi-Mod solution $\{\mathbf{u}_{m_\mathbf{u}}^{R,h}, p_{m_p}^{R,h}\}$ (from top to bottom: horizontal velocity, vertical velocity, pressure), with $\mathbf{u}_{m_\mathbf{u}}^{R,h} = [u_{m_\mathbf{u},1}^{R,h}, u_{m_\mathbf{u},2}^{R,h}]^T$.
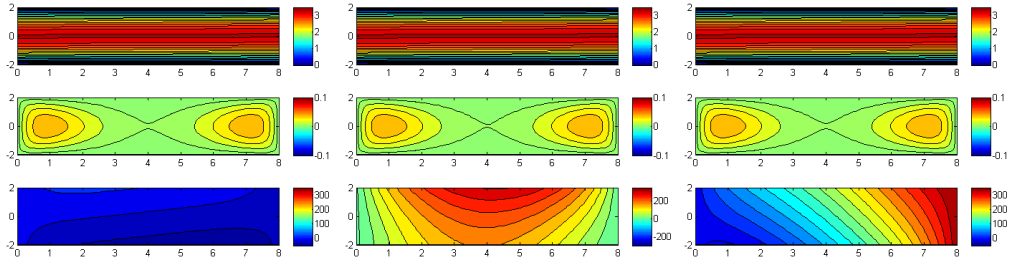

Figure 4: Steady Navier-Stokes equations. Hi-Mod reference solution (left), Hi-Mod approximation yielded by the monolithic Hi-POD approach for $l = 11$ (center) and $l = 28$ (right): horizontal (top) and vertical (middle) velocity components; pressure (bottom).

For the sake of completeness, we display the results of a monolithic approach in Figure 4 (center and right), where the POD basis is computed on a unique response matrix for the velocity and pressure. While velocity results are quite accurate, pressure approximation is bad, suggesting that, probably, a lack of inf-sup compatibility of the reduced basis leads to unreliable pressure approximations, independently of the dimension of the POD space.

When we turn to the segregated approach, Figure 5 shows the distribution of the singular values of the response matrices $R_{\mathbf{u}}$ and R_p, respectively. Again the values decay is not so rapid to pinpoint a clear cut-off value (at least for significantly small dimensions of the reduced basis), as a consequence of the multiple parametrization that inhibits the redundancy of the snapshots. However, when we compare the Hi-Mod solution identified by three different choices of the POD spaces, $V_{\text{POD}}^{l,\mathbf{u}}$ and $V_{\text{POD}}^{l,p}$, with the reference approximation in Figure 4 (left), we notice that the choice $l = 6$ is enough for a reliable reconstruction of the approximate solution (see Figure 6 (center)). The horizontal velocity component - being the most predominant dynamics - is captured even with a lower size of the reduced spaces $V_{\text{POD}}^{l,\mathbf{u}}$, while the pressure still represents the most challenging quantity to be correctly described.
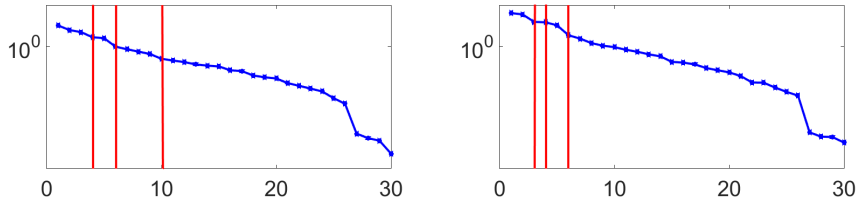

Figure 5: Steady Navier-Stokes equations. Singular values of the response matrix $R_{\mathbf{u}}$ (left) and R_p (right).
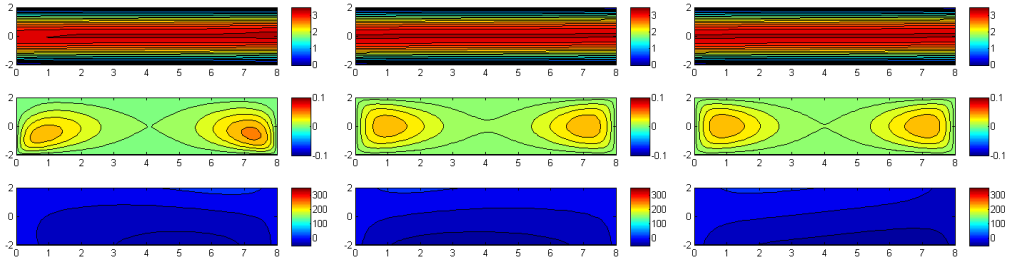

Figure 6: Steady Navier-Stokes equations. Hi-POD approximation yielded by the segregated Hi-POD approach for $l = 4$ (left), $l = 6$ (center), $l = 10$ (right): horizontal (top) and vertical (middle) velocity components; pressure (bottom).

In Table 2, we quantify the accuracy of the Hi-POD procedure. We compare the relative errors between the Hi-Mod reference solution $\{\mathbf{u}_{m_{\mathbf{u}}}^{R,h}, p_{m_p}^{R,h}\}$ and the Hi-POD approximation $\{\mathbf{u}_{m_{\mathbf{u}}}^{h}(\boldsymbol{\alpha}^*), p_{m_p}^{h}(\boldsymbol{\alpha}^*)\}$ generated by different Hi-POD schemes, with $\mathbf{u}_{m_{\mathbf{u}}}^{h}(\boldsymbol{\alpha}^*) = [u_{m_{\mathbf{u}},1}^{h}(\boldsymbol{\alpha}^*), u_{m_{\mathbf{u}},2}^{h}(\boldsymbol{\alpha}^*)]^T$.

As for the computational time (in seconds)[1], we found that the segregated Hi-POD requires $0.13s$ to be compared with $0.9s$ demanded by the standard Hi-

13

	$\dfrac{\|u_{m_{\mathbf{u}},1}^{R,h} - u_{m_{\mathbf{u}},1}^{h}(\boldsymbol{\alpha}^*)\|_{H^1(\Omega)}}{\|u_{m_{\mathbf{u}},1}^{R,h}\|_{H^1(\Omega)}}$	$\dfrac{\|u_{m_{\mathbf{u}},2}^{R,h} - u_{m_{\mathbf{u}},2}^{h}(\boldsymbol{\alpha}^*)\|_{H^1(\Omega)}}{\|u_{m_{\mathbf{u}},2}^{R,h}\|_{H^1(\Omega)}}$	$\dfrac{\|p_{m_p}^{R,h} - p_{m_p}^{h}(\boldsymbol{\alpha}^*)\|_{L^2(\Omega)}}{\|p_m^{R,h}\|_{L^2(\Omega)}}$
$l = 4$	$7.1 \cdot 10^{-3}$	$3.9 \cdot 10^{-1}$	$4.8 \cdot 10^{-1}$
$l = 6$	$3.8 \cdot 10^{-4}$	$4.3 \cdot 10^{-2}$	$3.9 \cdot 10^{-1}$
$l = 10$	$1.1 \cdot 10^{-4}$	$8.6 \cdot 10^{-3}$	$1.3 \cdot 10^{-3}$

Table 2: Steady Navier-Stokes equations. Relative errors for different Hi-POD reconstructions of the Hi-Mod solution.

Mod approximation. This highlights the significant computational advantage attainable by Hi-POD, in particular for a rapid approximation of the incompressible Navier-Stokes equations when estimating one or more parameters of interest.

4 Towards more realistic applications

We extend the Hi-POD segregated approach to the unsteady Navier-Stokes equations

$$
\begin{cases}
\dfrac{\partial \mathbf{u}}{\partial t}(\mathbf{x}, t) - \nabla \cdot (2\nu\, \mathbb{D}(\mathbf{u}))\,(\mathbf{x}, t) + (\mathbf{u} \cdot \nabla)\, \mathbf{u}(\mathbf{x}, t) + \nabla p(\mathbf{x}, t) = \mathbf{f}(\mathbf{x}, t) & \text{in } Q \\
\nabla \cdot \mathbf{u}(\mathbf{x}, t) = 0 & \text{in } Q \\
\mathbf{u}(\mathbf{x}, t) = \mathbf{0} & \text{on } G_D \\
(\mathbb{D}(\mathbf{u}) - p\mathbb{I})\,(\mathbf{x}, t)\, \mathbf{n} = g(\mathbf{x}, t)\mathbf{n} & \text{on } G_N \\
\mathbf{u}(\mathbf{x}, 0) = \mathbf{u}_0(\mathbf{x}) & \text{in } \Omega,
\end{cases}
\tag{12}
$$

$Q = \Omega \times I$ with $I = (0, T)$ the time window of interest, $G_D = \Gamma_D \times I$, $G_N = \Gamma_N \times I$, $\mathbf{u}_0$ the initial value, and where all the other quantities are defined as in (9). After introducing a uniform partition of the interval I into M subintervals of length Δt, we resort to the backward Euler scheme and approximate the nonlinear term via a classical first order semi-implicit scheme. The semi-discrete problem reads: for each $0 \leq n \leq M - 1$, find $\{\mathbf{u}^{n+1}, p^{n+1}\} \in V \equiv [H^1_{\Gamma_D}(\Omega)]^2 \times L^2(\Omega)$ such that

$$
\begin{cases}
\dfrac{\mathbf{u}^{n+1} - \mathbf{u}^n}{\Delta t} - \nabla \cdot \left(2\nu\, \mathbb{D}(\mathbf{u}^{n+1})\right) + (\mathbf{u}^n \cdot \nabla)\, \mathbf{u}^{n+1} + \nabla p^{n+1} = \mathbf{f}^{n+1} & \text{in } \Omega \\
\nabla \cdot \mathbf{u}^{n+1} = 0 & \text{in } \Omega \\
\mathbf{u}^{n+1} = \mathbf{0} & \text{on } \Gamma_D \\
\left(\mathbb{D}(\mathbf{u}^{n+1}) - p^{n+1}\mathbb{I}\right) \mathbf{n} = g^{n+1}\mathbf{n} & \text{on } \Gamma_N,
\end{cases}
\tag{13}
$$

with $\mathbf{u}^0 = \mathbf{u}_0(\mathbf{x})$, $\mathbf{u}^{n+1} \simeq \mathbf{u}(\mathbf{x}, t^{n+1})$, $p^{n+1} \simeq p(\mathbf{x}, t^{n+1})$ and $t^i = i\Delta t$, for $i = 0, \ldots, M$.

For the Hi-Mod approximation, we replace space V in (13) with the same Hi-Mod space as in the steady case.

When applied to unsteady problems, POD procedures are generally used for estimating the solution at a generic time by taking advantage of precomputed snapshots [26]. In our specific case, we know the Hi-Mod solution for a certain number of parameters $\boldsymbol{\alpha}_i$, and we aim at rapidly estimating the solution over a time interval of interest for a specific value $\boldsymbol{\alpha}^*$ of the parameter, with $\boldsymbol{\alpha}^* \neq \boldsymbol{\alpha}_i$. The procedure we propose here is the following one:

1. we precompute offline the steady Hi-Mod solution for p samples $\boldsymbol{\alpha}_i$ of the parameter, $i = 1, \ldots, p$;

2. for a specific value $\boldsymbol{\alpha}^*$ of the parameter, we compute online the Hi-Mod solution to (12) at the first times t^j, for $j = 1, \ldots, P$;

3. we juxtapose the Hi-Mod snapshots to the steady response matrix obtained offline;

4. we perform the Hi-POD procedure to estimate the solution to (12) at times t^j, with $j > P$.

In absence of a complete analysis of this approach, we present here some preliminary numerical results in a non-rectilinear domain. Hi-Mod reduction has been already applied to curvilinear domains [14, 17]. In particular, in [17] we exploit the isogeometric analysis to describe a curvilinear centerline Ω_{1D}, by replacing the 1D finite element discretization with an isogeometric approximation.

Here, we consider a quadrilateral domain with a sinusoidal-shaped centerline (see Figure 7). We adopt the same approach as in [14] based on an affine mapping of the bent domain into a rectilinear reference one. During the offline phase, we Hi-Mod solve problem (9) for $p = 5$ different choices of the parameter $\boldsymbol{\alpha} = [\nu, \mathbf{f}, g]^T$, by uniformly sampling the viscosity ν in $[1.5, 7]$, g in $[1, 80]$, and $\mathbf{f}(\mathbf{x}) = [f_1, f_2]^T$, with $f_1, f_2 \in \mathbb{R}$ in $[0, 10]$. Domain Ω_{1D} is divided in 80 uniform sub-intervals. We approximate $\mathbf{u}$ and p with five and three Legendre polynomials along the transverse direction combined with piecewise quadratic and linear functions along Ω_{1D}, respectively. The corresponding Hi-Mod approximations constitute the first p columns of the response matrices $R_{\mathbf{u}}$ and R_p.

Then, we solve the unsteady problem (12). We pick $\mathbf{u}_0 = \mathbf{0}$, $T = 10$, and we introduce a uniform partition of the time interval I, with $\Delta t = 0.1$. The data $\boldsymbol{\alpha}^*$ for the online phase are $\nu^* = 2.8$, $g^* = 30 + 20\sin(t)$ and $\mathbf{f}^* = [5.8, 1.1]^T$. Matrices $R_{\mathbf{u}}$ and R_p are added by the first $P = 5$ Hi-Mod approximations $\{\mathbf{u}_{m_{\mathbf{u}}}^{h,j}(\boldsymbol{\alpha}^*), p_{m_p}^{h,j}(\boldsymbol{\alpha}^*)\}$, for $j = 1, \ldots, 5$, so that $R_{\mathbf{u}} \in \mathbb{R}^{N_{\mathbf{u}} \times 10}$ and $R_p \in \mathbb{R}^{N_p \times 10}$, where $N_{\mathbf{u}} = 2 \times 5 \times N_{h,\mathbf{u}}$, $N_p = 3 \times N_{h,p}$ with $N_{h,\mathbf{u}}$ and $N_{h,p}$ the dimension of the one dimensional finite element space used along Ω_{1D} for $\mathbf{u}$ and p, respectively.

Figure 7 compares, at four different times, a reference Hi-Mod solution $\{\mathbf{u}_{m_{\mathbf{u}}}^{R,h}, p_{m_p}^{R,h}\}$, with $\mathbf{u}_{m_{\mathbf{u}}}^{R,h} = [u_{m_{\mathbf{u}},1}^{R,h}, u_{m_{\mathbf{u}},2}^{R,h}]^T$, computed by hierarchically reducing

problem (12) with the Hi-POD solution $\{\mathbf{u}_{m_\mathbf{u}}^h(\boldsymbol{\alpha}^*), p_{m_p}^h(\boldsymbol{\alpha}^*)\}$, with $\mathbf{u}_{m_\mathbf{u}}^h(\boldsymbol{\alpha}^*) = [u_{m_\mathbf{u},1}^h(\boldsymbol{\alpha}^*), u_{m_\mathbf{u},2}^h(\boldsymbol{\alpha}^*)]^T$, for $l = 6$. The agreement between the two solutions is qualitatively very good, in spite of the fact that no information from the Hi-Mod solver on the problem after time t^5 is exploited to construct the Hi-POD solution. The pressure still features larger errors, as in the steady case.

We make this comparison more quantitative in Table 3, where we collect the $L^2(\Omega)$- and the $H^1(\Omega)$-norm of the relative error between the Hi-Mod reference solution and the Hi-POD one, at the same four times as in Figure 7. We notice that the error does not grow significantly with time. This suggests that the Hi-POD approach can be particularly viable for reconstructing asymptotic solutions in periodic regimes, as in computational hemodynamics. As for the computational efficiency, Hi-POD solution requires $103s$ vs $287s$ of Hi-Mod one, with a significant reduction of the computational time.

	$\dfrac{\|u_{m_\mathbf{u},1}^{R,h} - u_{m_\mathbf{u},1}^h(\boldsymbol{\alpha}^*)\|_{H^1(\Omega)}}{\|u_{m_\mathbf{u},1}^{R,h}\|_{H^1(\Omega)}}$	$\dfrac{\|u_{m_\mathbf{u},2}^{R,h} - u_{m_\mathbf{u},2}^h(\boldsymbol{\alpha}^*)\|_{H^1(\Omega)}}{\|u_{m_\mathbf{u},2}^{R,h}\|_{H^1(\Omega)}}$	$\dfrac{\|p_{m_p}^{R,h} - p_{m_p}^h(\boldsymbol{\alpha}^*)\|_{L^2(\Omega)}}{\|p_{m_p}^{R,h}\|_{L^2(\Omega)}}$
$t = 2$	$5.4 \cdot 10^{-4}$	$4.5 \cdot 10^{-4}$	$3.4 \cdot 10^{-2}$
$t = 4$	$2.4 \cdot 10^{-3}$	$2.1 \cdot 10^{-3}$	$1.0 \cdot 10^{-1}$
$t = 6$	$2.3 \cdot 10^{-3}$	$2.2 \cdot 10^{-3}$	$6.2 \cdot 10^{-2}$
$t = T$	$2.6 \cdot 10^{-3}$	$2.4 \cdot 10^{-3}$	$7.7 \cdot 10^{-2}$

Table 3: Unsteady Navier-Stokes equations. Relative error associated with the Hi-Mod approximation provided by Hi-POD at different times.

5   Conclusions and future developments

The preliminary results in Sections 2.3, 3.1 and 4 yielded by the combination of the model/solution reduction techniques, Hi-Mod/POD, are very promising in view of modeling incompressible fluid dynamics in pipes or elongated domains. We have verified that Hi-POD enables a fast solution of parametrized ADR problems and of the incompressible, steady and unsteady, Navier-Stokes equations, even though in the presence of many (six) parameters. In particular, using Hi-Mod in place of a traditional discretization method applied to the reference (full) problem accelerates the offline phase and also the construction of the reduced problem projected onto the POD space.

Clearly, there are several features of this new approach that need to be investigated. First of all, we plan to migrate to 3D problems within a parallel implementation setting (in the library LifeV, www.lifev.org). Moreover, we aim at further accelerating the computational procedure by using empirical interpolation methods for possible nonlinear terms [23]. Finally, an extensive theoretical analysis is needed to estimate the convergence of the Hi-POD solution to the full one as well as the inf-sup compatibility of the Hi-Mod bases deserves to be rigorously analyzed.
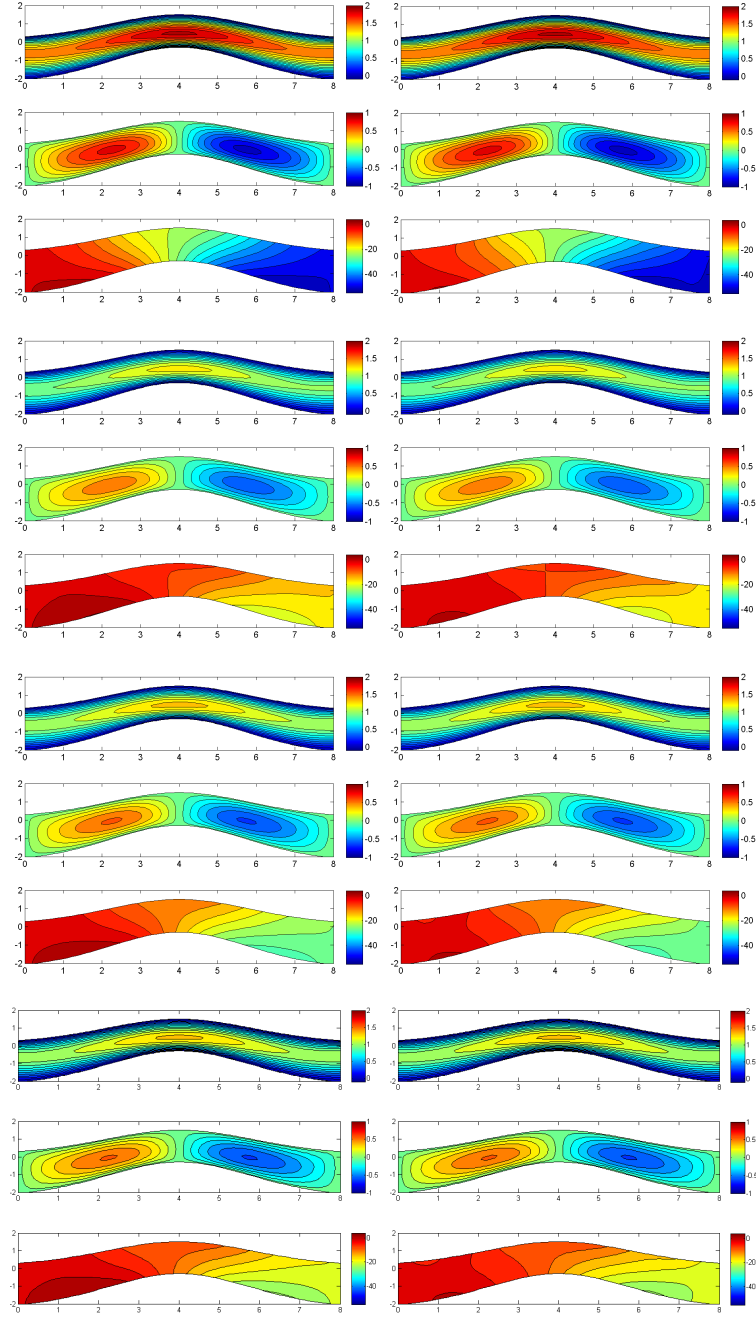
Figure 7: Unsteady Navier-Stokes equations. Reference Hi-Mod solution (left) and Hi-Mod approximation yielded by the Hi-POD approach for $l = 6$ (right), at $t = 2$ (first row), $t = 4$ (second row), $t = 6$ (third row) and $t = T$ (fourth row): horizontal (top) and vertical (middle) velocity components; pressure (bottom).

As reference application we are interested in computational hemodynamics, in particular to estimate blood viscosity from velocity measures in patients affected by sickle cell diseases [21].

Acknowledgments

References

[1] Aletti, M., Perotto, S., Veneziani, A.: Educated bases for the HiMod reduction of advection-diffusion-reaction problems with general boundary conditions. MOX Report no **37/2015**.

[2] Aletti, M.: Educated Bases for Hierarchical Model Reduction in 2D and 3D. Master Thesis in Mathematical Engineering, Politecnico di Milano, December 2013.

[3] Mansilla-Alvarez, L.A., Blanco, P.J., Bulant, C., Dari, E., Veneziani, A., Feijoo, R.: Pipe-oriented hybrid finite element approximation in blood flow problems. Accepted for the publication in Int. J. Numer. Meth. Biomed. Eng. (2016).

[4] Ern, A., Perotto, S., Veneziani, A.: Hierarchical model reduction for advection-diffusion-reaction problems. In: Kunisch, K., Of, G., Steinbach, O. (eds.). Numerical Mathematics and Advanced Applications, pp. 703–710. Springer-Verlag, Heidelberg (2008).

[5] Guzzetti, S., Perotto, S., Veneziani, A.: Hierarchical Model reduction solvers for the incompressible Navier-Stokes equations in cylindrical coordinates. In preparation, 2016.

[6] Golub, G.H., Van Loan, C.F.: Matrix Computations. Johns Hopkins University Press, Baltimore (2013), fourth edition.

[7] Gunzburger, M.D.: Perspectives in Flow Control and Optimization. Advances in Design and Control, **5**. Society for Industrial and Applied Mathematics (SIAM), Philadelphia (2003).

[8] Hinze, M., Volkwein, S.: Error estimates for abstract linear-quadratic optimal control problems using proper orthogonal decomposition. Comput. Optim. Appl. **39**(3), 319 –345 (2008).

[9] Huanhuan, Y., Veneziani, A.: Efficient estimation of cardiac conductivities via POD-DEIM model order reduction. http://arxiv.org/abs/1603.05722

[10] Kahlbacher, M., Volkwein, S.: Galerkin proper orthogonal decomposition methods for parameter dependent elliptic system. Discuss. Math. Differ. Incl. Control Optim. **27**, 95–17 (2007).

[11] Lions, J.-L., Magenes, E.: Non Homogeneous Boundary Value Problems and Applications. Springer, Berlin (1972).

[12] Lupo Pasini, M.: HI-POD: HIerarchical Model Reduction Driven by a Proper Orthogonal Decomposition for Advection-Diffusion-Reaction Problems. Master Thesis in Mathematical Engineering, Politecnico di Milano, December 2013.

[13] Lupo Pasini, M., Perotto, S., Veneziani, A. In preparation, 2016.

[14] Perotto., S.: Hierarchical model (Hi-Mod) reduction in non-rectilinear domains. In: Erhel, J., Gander, M., Halpern, L., Pichot, G., Sassi, T., Widlund, O. (eds.). Domain Decomposition Methods in Science and Engineering. Series: Lect. Notes Comput. Sci. Eng., Vol. **98**, pp. 477–485, Springer, Cham (2014).

[15] Perotto, S.: A survey of Hierarchical Model (Hi-Mod) reduction methods for elliptic problems. In: Idelsohn, S.R. (ed.). Numerical Simulations of Coupled Problems in Engineering. Series: Computational Methods in Applied Sciences, Vol. **33**, pp. 217–241, Springer, Cham (2014).

[16] Perotto, S., Ern, A., Veneziani, A.: Hierarchical local model reduction for elliptic problems: a domain decomposition approach. Multiscale Model. Simul. **8**(4), 1102–1127 (2010).

[17] Perotto, S., Reali, A., Rusconi, P., Veneziani A.: HIGAMod: a Hierarchical IsoGeometric Approach for MODel reduction in curved pipes. Accepted for the publication in Comput. & Fluids (2016).

[18] Perotto, S., Veneziani, A.: Coupled model and grid adaptivity in hierarchical reduction of elliptic problems. J. Sci. Comput. **60**(3), 505–536 (2014).

[19] Perotto, S., Zilio, A.: Hierarchical model reduction: three different approaches. In: Cangiani, A., Davidchack, R.L., Georgoulis, E., Gorban, A.N., Levesley, J., Tretyakov, M.V. (eds.). Numerical Mathematics and Advanced Applications, pp 851–859. Springer-Verlag, Berlin Heidelberg (2013).

[20] Perotto, S., Zilio, A.: Space-time adaptive hierarchical model reduction for parabolic equations. Adv. Model. and Simul. in Eng. Sci. **2**(25), 1–45 (2015).

[21] Rivera, C.P., Veneziani, A., Ware, R.E., Platt, M.O.: Sickle cell anemia and pediatric strokes: computational fluid dynamics analysis in the middle cerebral artery. Exp. Biol. Med. (Maywood), 2016 Apr 4; **241**(7), 755–65. Epub 2016 Mar 4, doi:10.1177/1535370216636722

[22] Quarteroni, A., Saleri, F., Veneziani, A.: Factorization methods for the numerical approximation of Navier-Stokes equations. Comput. Methods Appl. Mech. Engrg. **188**(1-3), 505–526 (2000).

[23] Rozza, G., Hesthaven, J.S., Stamm, B.: Certified Reduced Basis Methods for Parametrized Partial Differential Equations. SpringerBriefs in Mathematics. BCAM SpringerBriefs. Springer, Cham (2016).

[24] Elman, H.C., Silvester, D.J., Wathen, A.J.: Finite Elements and Fast Iterative Solvers: with Applications in Incompressible Fluid Dynamics. Numerical Mathematics and Scientific Computation. Oxford University Press, Oxford, (2014), second edition.

[25] Temam, R.: Navier-Stokes Equations. Theory and Numerical Analysis. North-Holland Publishing Co., Amsterdam (1984), third edition.

[26] S. Volkwein. Proper Orthogonal Decomposition: Theory and Reduced-Order Modelling. Lecture Notes, University of Konstanz (2013).

[27] Veneziani, A., Villa, U.: ALADINS: an ALgebraic splitting time ADaptive solver for the Incompressible Navier-Stokes equations. J. Comput. Phys. **238**, 359–375 (2013).

[28] Veneziani, A., Viguerie, A.: Algebraic splitting methods for the steady incompressible Navier-Stokes equations. In preparation, 2016.

MOX Technical Reports, last issues

Dipartimento di Matematica
Politecnico di Milano, Via Bonardi 9 - 20133 Milano (Italy)

24/2016   Pagani, S.; Manzoni, A.; Quarteroni, A.
A Reduced Basis Ensemble Kalman Filter for State/parameter Identification in Large-scale Nonlinear Dynamical Systems

23/2016   Fedele, M.; Faggiano, E.; Dedè, L.; Quarteroni, A.
A Patient-Specific Aortic Valve Model based on Moving Resistive Immersed Implicit Surfaces

22/2016   Antonietti, P.F.; Facciola', C.; Russo, A.;Verani, M.
Discontinuous Galerkin approximation of flows in fractured porous media

21/2016   Ambrosi, D.; Zanzottera, A.
Mechanics and polarity in cell motility

19/2016   Guerciotti, B.; Vergara, C.
Computational comparison between Newtonian and non-Newtonian blood rheologies in stenotic vessels

20/2016   Wilhelm, M.; Sangalli, L.M.
Generalized Spatial Regression with Differential Regularization

Guerciotti, B.; Vergara, C.
Computational comparison between Newtonian and non-Newtonian blood rheologies in stenotic vessels

18/2016   Ferroni, A.; Antonietti, P.F.; Mazzieri, I.; Quarteroni, A.
Dispersion-dissipation analysis of 3D continuous and discontinuous spectral element methods for the elastodynamics equation

17/2016   Penati, M.; Miglio, E.
A new mixed method for the Stokes equations based on stress-velocity-vorticity formulation

15/2016   Ieva, F.; Paganoni, A.M.
A taxonomy of outlier detection methods for robust classification in multivariate functional data